J Nanostruct 14(3): 875-892, Summer 2024

RESEARCH PAPER

Eco-Friendly of Nano-Nickel Oxide Particles Using Garlic Extract: Characterization, and Surface Coating

Oum Kalthoum Yousefi, Esmaiel Soleimani *

Inorganic Chemistry Research Laboratory, Faculty of Chemistry, Shahrood University of Technology, Shahrood, Iran

ARTICLE INFO

Article History:
Received 13 April 2024
Accepted 21 June 2024
Published 01 July 2024

Keywords:
Garlic extract
Nano-NiO particles
Photocatalytic deactivation
Surface coating

ABSTRACT

The nano-nickel oxide particles have been prepared by the biosynthesis method from a reaction of $Ni(NO_3)_2.6H_2O$ with the help of Phyto-constituents present in the garlic extract solution as both capping and stabilizing agents, and heating sediment at 400 °C for five hours. The surface of nano-NiO particles was rectified by palmitic and stearic acids. The change of property of hydrophobic of coated nano-NiO particles was proved via lipophilic degree (LD) tests. These results proved that the LD of the coated nano-NiO particles increased with increasing the rectifier values to up to 5.0 wt%. Optimal surface coating of nano-NiO particles was also achieved at 35 °C during a reaction time of 150 min. The coated nano-NiO particles were identified by XRD pattern, EDX and FT-IR spectra, TGA analysis, and SEM images. The results showed that the chains of palmitic and stearic acids have been effectively connected onto the surface of nano-NiO particles and that percentage of grafting can reach 2.1 and 2.7 wt% respectively. The SEM images show a good dispersity after the coating of nano-NiO particles by fatty acids. This betterment in the dispersal of nano-NiO particles indicated that grafted chains of fatty acids on nano-NiO particles could markedly prevent aggregation of nano-NiO particles in acetone and liquid paraffin. The photocatalytic behavior of improved nano-NiO particles was also investigated for the destruction of methyl orange (MO). The results proved that catalytic destruction of nano-NiO particles decreases when anchored by palmitic and stearic acids.

How to cite this article
Yousefi O., Soleimani E. Eco-Friendly of Nano-Nickel Oxide Particles Using Garlic Extract: Characterization, and Surface Coating. J Nanostruct, 2024; 14(3):875-892. DOI: 10.22052/JNS.2024.03.017

INTRODUCTION

The distribution of electrons in orbitals, optical absorption behavior, and electron charge mutation properties of often metallic oxides and sulfides make them feasible to use as a photocatalyst [1-6]. Nanoparticles of metal sulfides and oxides are usually prepared by materials that include solvents, reducing agents, and inorganic and organic compounds. Sol-Gel technique [7, 8], precipitation and co-precipitation reactions [9-11], thermal decomposition [12-14], hydrothermal route [9, 15, 16], microwave-assisted polyol method [17], green route [18], and ship-in-a-bottle procedure [19], are some of the routes involved for synthesizing nanostructured metal oxides and sulfides for different applications.

Phyto-synthesis of nanoparticles using the green method is a newfangled technique that has gained more attention in recent years going to its accessibility, low cost, and eco-friendly

* *Corresponding Author Email: essoleimani@shahroodut.ac.ir*

over the formal chemical-physical methods [20]. The use of plant extract is generating interest from researchers in the cost-effective and eco-friendly green synthesis of nanoparticles. For example, CuO NPs were synthesized using coffee powder extracts by the sol-gel method at different calcination temperatures [21].

Green syntheses are required to avoid the production of unwanted or harmful by-products through the build-up of reliable, sustainable, and eco-friendly synthesis procedures. The use of ideal solvent systems and natural resources (such as organic systems) is essential to achieve this goal [22]. Typically, CuO NPs synthesized by an implicitly environmentally benign process using *Acanthospermum hispidum* L. aqueous plant extract as an effective bio-oxidizing/bio-reducing agent. Phytochemical screening of the fresh aqueous leaves extract showed the presence of coumarins, tannins, saponins, phenols, flavonoids, sterols, and volatile oils. CuO NPs evinced highly robust antimicrobial, antimalarial, and antimycobacterial activity [23].

Green synthesis methodologies based on biological precursors depend on various reaction parameters such as solvent, temperature, pressure, and pH conditions (acidic, basic, or neutral) [24]. Modi et al. reported the green synthesis of ZnO NPs by Allium sativum skin (garlic skin) extract. The ZnO NPs synthesized using garlic skin are expected to have applications in biotechnology, biomedical, catalysis, coatings, sensors, and water remediation [25].

For the synthesis of metal/metal oxide NPs, plant biodiversity has been broadly considered due to the availability of effective phytochemicals in various plant extracts, especially in leaves such as ketones, aldehydes, flavones, amides, terpenoids, carboxylic acids, phenols, and ascorbic acids. These components are capable of reducing metal salts into metal NPs [26, 27]. Phytochemicals in garlic extract can play the role of reduction of metal ions and capping for nanoparticles, thus leading to green synthesis. Garlic (*Allium sativum L.*) includes a wide range of materials, such as sulfur and polyphenolic compounds, which have advantages for human health. Both phenolic and sulfur compounds take part in antioxidant activity in *Allium* species [28-30].

The biosynthesis of oxide semiconductor NPs using materials found in nature opens a wide field of study focused on sustainability and environmental protection. Biosynthesized NPs can eliminate organic dyes, which pollute water and cause severe damage to the environment. The green synthesis of zinc oxide (ZnO) NPs was carried out using *Capsicum annuum var. Anaheim* extract [31].

The surface of inorganic compounds like metallic oxides is polarized and that's why they have a water-loving character. They, so, have a minor inclining to dispersity in an organic solvent that restricts their utilization of them in organic media [32]. A good route to vin these restrictions is the coating of nano-inorganic compounds with organic and bioinorganic molecules.

Fatty acids were used as a modifier for surface modification of NPs that are being developed. For example, Wang *et al.* coated the surface of nano-calcite and nano-alumina with lauric acid. Then the degree of activation of NPs as well as the volume of sedimentation was measured for them. The results showed that by increasing the degree of activation, sedimentation volume was reduced; the hydrophilic character of the nanomaterials inorganic changed to hydrophobic [33].

A green and facile approach to the efficient surface modification of alumina and other metal oxide NPs with fatty acids has been proposed. Only water was used as the dispersing medium, the modified metal oxide NPs were automatically separated from water, and water can be recycled. The modification efficiency, using oleic acid as an example, of this water-alone method was 36% higher than that of the water-ethanol method. The modification efficiency increases with increasing chain length of the fatty acids [34].

A novel superhydrophobic alumina surface is fabricated by grafting a stearic acid layer onto the porous and roughened aluminum film. Results show that a super water-repellent surface with a contact angle of 154.2° is generated. Furthermore, the roughened and porous alumina surface is coated with a layer of hydrophobic alkyl chains which come from stearic acid molecules. Therefore, both the roughened structure and the hydrophobic layer endue the alumina surface with the superhydrophobic behavior [35].

Covering the surface of NPs tends to create different chemical and physical properties on their surfaces. For example, when the surface of ZnO NPs coated using oleic acid *via* covalent bonds resulting from the reaction of hydroxyl groups on the superficial and hydrogen of the carboxylic

acid groups. The stability of ZnO NPs in the organic matrix increases and this, in turn, will increase the dispersibility [36-38]. The photocatalytic activity of nano-ZnO coated using SiO_2 greatly decreases due to the protective layer [36].

The silane-modified ZnO NPs showed strong hydrophobicity and good compatibility with organic media, as well as remarkably reduced photocatalytic operation [39]. Yu et al. proposed a facile method for the preparation of superhydrophobic chitosan composite films by deposition of ZnO NPs, followed by stearic acid modification. The wettability of the chitosan films was a function of the film surface roughness and the low surface energy of stearic acid. Importantly, the chitosan composite film had high resistance to water droplets, low adhesion, good stability, long-term durability, and excellent oil–water separation capacity [40].

Different surface treatments including stearic acid, mercerization, and growth of ZnO nanorods as well as their combinations were exploited to address their effects on the properties of green composites based on polylactic acid (PLA) and flax fabrics. The tensile and flexural properties of composites produced by compression moulding were significantly influenced. The presence of ZnO nanorods promoted an increase in flexural and tensile stiffness by 58% and 31%, respectively [41].

A superhydrophobic coating material (PA-ZnO) with a static water contact angle (WCA)>160° has been synthesized by modifying ZnO NPs with palmitic acid (PA). ZnO NPs (size ~ 24 nm) with hexagonal wurtzite structure are prepared by hydrothermal method. This superhydrophobic nature of PA-ZnO has been attributed to the grafting of palmitic acid on the ZnO surface which is confirmed by conducting the WCA measurement of PA-ZnO samples after heating at different temperatures [42].

Nam and his coworker also used stearic acid for the surface coating of nano-TiO_2. The surface treatment makes nano-TiO_2 hydrophobic with a contact angle of 119° [43]. The surface of nano-TiO_2 particles was coated using 3-aminopropyltrimethoxysilane and 3-isocyanatopropyl trimethoxysilane in an aqueous process. The rate constant of TiO_2 photocatalytic activity for degradation of the malachite green solution was decreased by increasing the organosilane ratio up to 20 %wt [44].

2D Janus sheets with stearic acid at one side and TiO_2 at the other side of the same plane, which was called vertical STA-TiO_2 Janus sheets (V-STA-TiO_2 JNs), were prepared via a simply and easily operated impregnation method. Dispersion behavior and contact angle both demonstrated that V-STA-TiO_2 JNs were amphiphilic. V-STA-TiO_2 JNs can be used as an emulsifier to prepare Pickering emulsion and existed vertically at the oil–water interface observed by a polarized optical microscope. V-STA-TiO_2 JNs showed higher catalytic activity in the photocatalytic degradation of nitrobenzene (NB) and kerosene in wastewater [45].

Hydrophobic Co_3O_4 NPs with excellent surface self-cleaning were made by surface modification using stearic acid. The results showed that after surface modification the hydrophobic character of NPs is excellent with a contact angle of 155 °, and is stable at pH between 3.0 and 14.0 [46].

The nano-CuO particles are prepared by chemical precipitation and followed by the heating of sediment at 500 °C. The surfaces of nano-CuO particles were coated using stearic acid. The experimental results displayed the photocatalytic destruction of MO was reduced when nano-CuO particles were coated by stearic acid [47].

The development of nano lubricants has increased rapidly in recent years. With the addition of nano-additives to conventional oils to enhance tribological properties, the stability of NPs remains a challenge, which can be ruled out with the help of surface modification of nanoparticles. So, surfaces of metal oxide NPs (Al_2O_3, CuO, and SiO_2) are done with the help of oleic acid (OA) [48].

Among oxides, nickel oxide has been very much considered owing to its usage in a lot of fields, like catalysis, magnetic materials, gas sensors, photovoltaic devices, and fuel cells [49-53]. The nanostructured nickel oxide has many usages as a p-type semiconductor and a stable wide-band gap (3.11–3.86 eV) [54, 55].

Adding carbon compounds such as activated carbon (AC), graphene oxide (GO), and reduced graphene oxide (RGO) to nano-NiO particles increases its photocatalytic activity. For example, A modest hydrothermal approach is adopted to build NiO/RGO NCs. It exhibited remarkable photocatalytic behavior for the destruction of MO, demonstrating that MO has a degradation efficiency of 50 min 99.9% [56]. NiO/RGO nanocomposites were prepared through an optimized hydrothermal method. The bandgap

of nano-nickel oxide particles decreased after incorporation with RGO. NiO/RGO nanocomposites show more suitable photocatalytic performance to remove RhB dye. NiO/RGO nanocomposites had the highest rate constant of 0.016 min^{-1}, which is about 1.5 times higher than nano-NiO particles [57].

AC-supported nano-NiO particles were prepared to utilize thermal decomposition. These AC-NiO composites (NCs) were stabilized on alginate layers to obtain the 3D network structure of Alg@AC-NiO NCs layers. These NCs were utilized for the catalytic reduction of Congo red (CR) dye. The revival of CR was investigated under the influence of $NaBH_4$ concentration, catalyst dosage, and CR dye concentration. Statistical modeling of optimal catalytic conditions for $NaBH_4$ of 0.05 M, catalyst of 11 mg, and CR of 80 ppm was obtained, which resulted in 99.67% of CR conversion [58].

While the addition of some other carbon compounds such as fatty acids to NiO NPs lowers its photocatalytic activity [59]. The organic surface modifiers are particularly preferred, to deactivate the photocatalytic of nano-NiO particles. Fatty acids have special significance for the deactivation of nano-NiO particles. Therefore, the surface of nano-NiO particles has been modified using fatty acids to realize photocatalytic deactivation and promote organic layer compatibility of nano-NiO particles. They will act as UV-shielding compounds in cosmetics and sanitary. Because of this, stearic and palmitic acids were used for the surface coating of nano-NiO particles. It is hoped that this will remarkably reduce the photocatalytic activity of nano-NiO particles and increase their compatibility with organic media in sunscreen sanitary and cosmetics.

In continuation of our previous work [60, 61], here are reported nano-NiO particles prepared by green route from the reaction of $Ni(NO_3)_2.6H_2O$ with garlic extract as reducing and stabilizing parameters, and then the heating of sediment at 400 °C for five hours.

To date, the preparation of nano-NiO particles by garlic extract has not been reported. It seems that the Phyto-synthetic method of nano-NiO particles is low-cost and promises an alternative to conventional methods. Among the advantages of the preparation method in this research work: Extraction from garlic cloves is a cheap and accessible material, extraction is a simple and easy method to prepare a natural and harmless reducing, and using the extract instead of a potentially dangerous and toxic chemical such as hydrazine, sodium borohydride, etc.

The surfaces of as-prepared nano-NiO particles were then coated using stearic and palmitic acids. The bare nano-NiO particles and their modifications were confirmed by EDX and FT-IR spectra, XRD patterns, TGA analysis, and SEM images. The optimal conditions including the amount of modifier, time, and temperature reaction were measured by determining the LD of modified nano-NiO particles. The dispersion of surface-coated nano-NiO particles in an organic solvent and their photocatalytic deactivation were tested for the destruction of MO aqueous.

MATERIALS AND METHODS

Chemicals and Methods

In the present project, compounds like $Ni(NO_3)_2.6H_2O$, ethanol, palmitic acid, stearic acid, chloroform, methanol, methyl orange, paraffin, and acetone were purchased from Aldrich and Merck.

The XRD patterns were achieved on the D8-Brucker, and the UV-Visible spectroscopy was recorded by Shimadzu UV-160 spectrophotometer. The EDX analysis of the compound was done with the help of JEOL JSM-7600F for composition analysis. The surface morphology of nanoparticles and nanocomposite were investigated by SEM, Hitachi Japan, S4160, and the FT-IR diagrams were investigated on FT-IR Rayleigh WQF-510 spectrophotometer. The thermogravimetric curve was done on a TG-209 thermoanalyzer with a rate of 10 ºC/min. The photocatalytic performance of particles was studied with the ultraviolet light of a mercury lamp of 50 Watts. A thermal furnace of Raypa by an HM-9 model was utilized for annealing particles.

Synthesis and surface modification of nano-NiO

Garlic cloves were peeled and washed with water to eliminate any contamination. Garlic extract was got by crushing 20 g of garlic cloves in 200 mL of water with the help of a mortar and pestle. The extract was then filtered and the filtrate was stored in the refrigerator for later use.

Aqueous extract of garlic was added to 50 mL of $Ni(NO_3)_2 \cdot 6H_2O$ 0.1 M along with stirring for 20 min. This mixture was stirred vigorously for two hours at 70 °C until reduced to a light green paste. The paste was heated at 400 °C for five hours to get

nano-NiO particles.

For surface modification of NPs typically, 1.0 g of nano-NiO particles were subjoined to a solution of 100 mg stearic acid (and or palmitic) in 15 mL $CHCl_3$. The reaction mixture was stirred at 35 °C for four hours. The coated nano-NiO particles separated, washed twice with 10 mL $CHCl_3$ and dried at 90 °C for 30 h.

Antioxidant function

The antioxidant performance of garlic extract was determined by the DPPH method. First, 5.0 mL of 0.004% DPPH in ethyl alcohol was added to various amounts (100, 200, 300, 400, and 500 mg/L) of garlic extract. These mixtures were shaken vigorously and incubated in the dark for 45 minutes.

The absorbency of the arouses solution was determined at a wavelength of 517 nm. The ascorbic acid (4.0 g in 10.0 ml water) was utilized as a standard solution. A decrease in the absorption of the solution proved a higher percentage of the inhibition performance. The inhibitory action of DPPH is determined by Eq. 1:

$$\% \text{ Inhibition} = \frac{(A_b - A_s)}{A_b} \times 100 \quad (1)$$

Where A_s and A_b is the absorbency of the extract and blank solution, respectively.

The measure of the lipophilic degree

A route to determine the LD of the surface of particles to disperse a specified number of modified nanoparticles in water and titrates by an organic compound such as ethanol and or methanol [60, 61]. When bare nano-NiO particles are poured into water, the precipitate is formed rapidly, whereas the coated nano-NiO particles by stearic and palmitic acids float on the surface of the water. By pouring methanol dropwise into a dispersed solution of coated nano-NiO particles (20 mg/ 20.0 mL of water), the coated particles gradually formed sediment. By measuring the content of methanol consumed, the LD of coated particles calculated by Eq. 2:

$$\text{LD} = \frac{V}{(V+10)} \times 100 \quad (2)$$

Where, V is the content of methanol consumed in mL, and 10 is the primary content of water in suspension. The LD of coated nano-nickel oxide particles is due to various amounts of stearic and palmitic acids was determined by the upper procedure. The measure of LD was employed as a way to evaluate the surface coating process.

Dispersibility in organic media

A certain amount of coated nano-NiO particles (2.5, 5, 10, 15, 20 %wt) was dispersed in each of the solvents of acetone, ethanol, and liquid paraffin (10.0 mL), and subjected to ultrasonic waves for 45 min. These samples were then allowed to remain in the laboratory for 72 hours without shaking, after which the particles in suspension were precipitated. The sediment was centrifuged and dried at 65 °C for 30 hours. The mass of stable particles in the dispersed suspension was measured by the gravimetric method (%wt).

Photocatalytic deactivation

Various reports and experiments have shown that the nano-NiO particles have a low energy gap with semiconductor properties, and this behavior allows them to destroy dyes and pigments such as methylene blue, methyl red, and methyl orange [62-67].

In our experiments, nano-NiO particles and also their modified photocatalyst (50 mg) was added to 100 mL of MO (20 ppm), and the reaction mixture was stirred and radiated in a photoreactor. The mixture was kept in darkness for 45 min before UV irradiation was produced from a 50 W mercury lamp.

Then, after every two hours of irradiation on the reaction mixture, 5.0 mL was withdrawn and the suspended particles were separated by centrifugation (3500 rpm at 15 min) and the absorbency of the solution was recorded at 464 nm. At last, the photocatalytic destruction percentage (PDP) of nano-NiO particles and their modification were determined according to Eq. 3:

$$\% \text{ PDP} = \frac{(A_0 - A_t)}{A_0} \times 100 \quad (3)$$

Where A_t is the absorbency of the MO at time t, A_0 is the initial absorbency. In the same way, the PDP of the coated nano-NiO particles by stearic acid was investigated with various amounts of modifiers (2.5, 5, 7.5, 10, 12.5, and 15 % wt), and the efficiency of destruction was determined.

RESULT AND DISCUSSION

For the first time, the nano-NiO particles were prepared using an environmentally friendly strategy

and the use of garlic extract. Aqueous extract of garlic has rich sources of active species such as organosulfur compound L-cysteine peptides, L-cysteine sulfoxides, flavonoids, polyphenols, allicin, alkaloids, and proteins. The phenolic compounds have a desirable effect on the synthesis of nanoparticles. Hydroxyl groups of polyphenols and ketone groups(C=O) of flavonoids bonded with metal ions and form stable coordination compounds [68]. These compounds decompose directly at high temperatures and form metallic oxide particles.

In the present work, the polyphenols present in the garlic extract with the loss of hydrogen ion converted stable nickel-phenolate coordination. Next, the resulting compound is decomposed at 400 °C in the calcination process and nickel oxide nanoparticles are formed.

Separately nickel oxide NPs interact with up to two surface modifiers, namely stearic and palmitic acids. In a condensation process, the carboxyl groups of stearic and palmitic acids interact with the hydroxyl groups on the surface of nano-nickel oxide particles, as such the fatty acids bind to the nickel oxide NPs. As a result, the surface of nano-NiO particles was coated by two suitable coatings (palmitic acid and stearic acid). Fig. 1 displays the surface coating of nano-NiO particles using palmitic and stearic acids.

Antioxidant assay

The antioxidant performance of plant extracts includes phenolic compounds due to their ability to donate free electrons and hydrogen atoms. DPPH free radical test is a suitable way to detect the antioxidant behavior of substances. The mechanism of this behavior includes a hydrogen atom transfer as well as an electron transfer. 2,2-diphenyl-1-picrylhydrazyl is a sustainable active radical whose purple changes to yellow in the vicinity of antioxidants.

The DPPH experiments show that garlic extract has a considerable antioxidant futuristic. This behavior happens due to a shortage of hydrogen or electron acceptors. The reducing capability of garlic extract was determined by spectrophotometric analysis by an absorption band at 517 nm due to the change in the color of DPPH from purple to yellow [69]. Inhibition was high in garlic extract because garlic acts as a well antioxidant that can lose electrons. The DPPH experiments displayed effectively free radical deterrence by garlic extract (Table 1). These results displayed that as the concentration of the extract increases, the absorption of its solution at 517 nm decreases, which means that the inhibition of DPPH radicals has occurred. Electrons present in plant chemicals are paired in the vicinity of a radical scavenger. In this condition, absorption is lost, and the radical

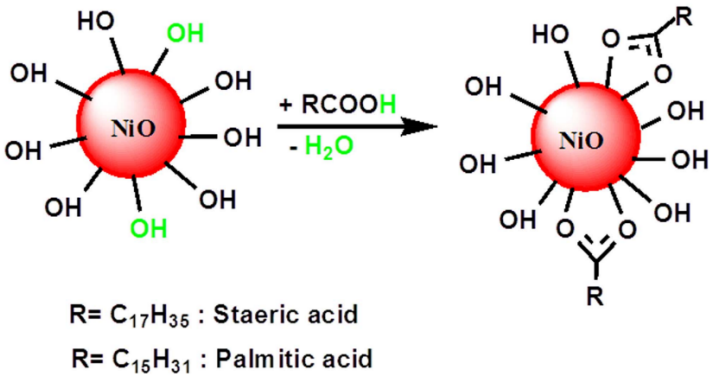

Fig. 1. The surface coating of nano-NiO particles by stearic acid and palmitic acid.

Table 1. Potential of garlic extract for inhibition of PDDH radical.

Concentration [ppm]	100	200	300	400	500
Scavenge of DPPH [%]	41	46	50	62	74

changes color [70]. An antioxidant effort stops oxidation by neutralizing the free radicals formed. Antioxidants themselves go through oxidation to deactivate free radicals [71]. Therefore, garlic extract can act as a stabilizing and reducing species to prepare nano-metal particles and nano-metal oxide particles.

FT-IR Spectra

Examination of broken chemical bonds, as well as bonds formed in the coating process, the FT-IR analysis of nano-nickel oxide particles, were recorded in the surface coating by stearic and palmitic acids. The FT-IR spectrum of nano-nickel oxide particles formed by the garlic extract is illustrated in Fig. 2.

The strong band observed at the lower frequency, at 480 cm^{-1}, can be imputed to the stretching frequency of the nickel-oxygen bond [71, 72]. The bands observed in regions 3450, 3125, 2930, 2850, 1625 and 1460 cm^{-1} can be imputed to the O-H phenol, C-H aromatic, C-H aliphatic, carbonyl, and C=C aromatic functional groups present in the garlic extract [73-76]. These functional groups indicate the presence of polyphenols in garlic extract. The phytochemicals of garlic extract remain on the surface of nickel oxide nanoparticles and these materials are separated by heat at 400 °C.

These FT-IR spectra are displayed in Fig. 3. A band at 484 cm^{-1} of bare nano-NiO particles (Fig. 3a) may be imputed to the stretching frequency of

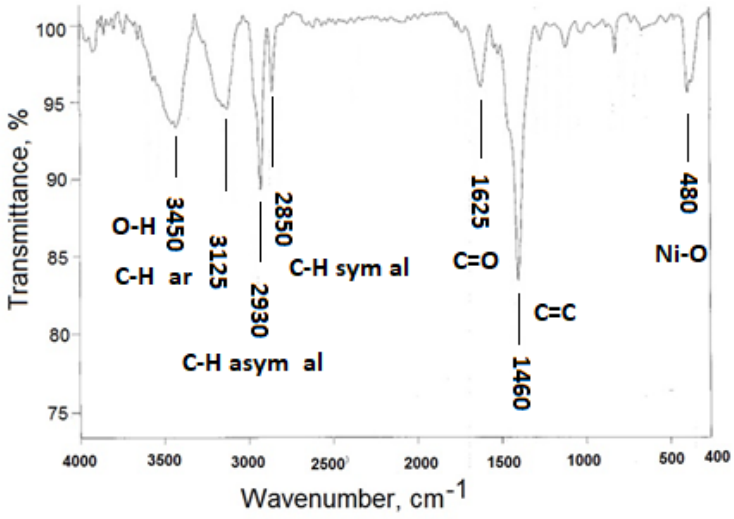

Fig. 2. The FT-IR analysis of nano-NiO particles formed by the garlic extract.

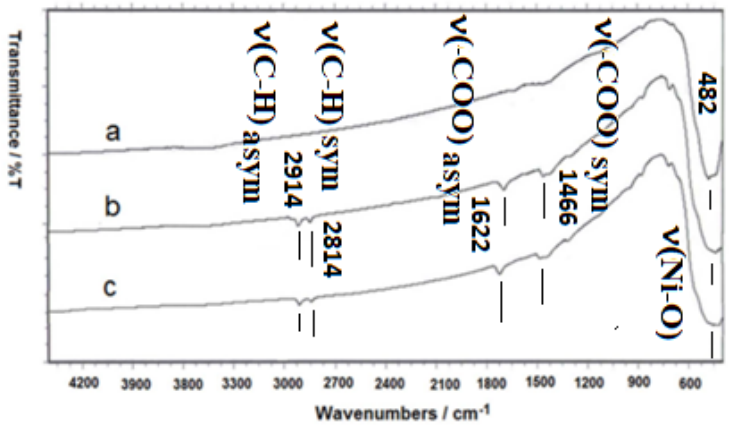

Fig. 3. FT-IR analysis of (a) nano-NiO particles; (b) nano-NiO

Ni-O in nickel oxide [77]. While in the FT-IR spectra of nano-NiO particles coated using stearic acid (Fig. 3b) and palmitic acid (Fig. 3c), in addition to the nickel-oxygen vibration band, other bands are observed in the region of 2914, 2814, 1622 and 1466 cm^{-1}.

The bands at 2914 and 2846 cm^{-1} belong to stretching frequencies of the CH_3 and CH_2 group of fatty acids coating on the surface of nano-NiO particles [33, 47]. The other two bands at 1466 and 1622 cm^{-1} may be attributed to symmetric and asymmetric vibrations of the carboxylate half of the fatty acids that coated the surface of nano-NiO particles respectively [78, 79]. The difference bands at about 156 cm^{-1} confirm that the carboxylate (-COO-) acts as a bidentate chelate and is grafted to the surface of nano-NiO particles [36, 47]. The observations of these four bands in infrared confirm that the surface of nano-NiO particles was coated by stearic and palmitic acids.

XRD patterns

X-ray diffraction pattern of nano-nickel oxide particles was recorded for surface coating using stearic and palmitic acids, and outcomes are displayed in Fig. 4.

The special angles with 2θ of 37.2, 43.3, 62.8, 75.2, and 79.4 º correspond to the cubic crystal of nickel oxide and lattice parameter a= 4.193 Å. It fits well with the standard card of JCPDS-04-0835 [61, 80, 81]. These angles are attributed to the diffraction of crystal sheets of (111), (200), (220), (311), and (222) of the FCC phase of nickel(II) oxide respectively. Other signals were not observed, so nickel oxide nanoparticles with high purity were prepared.

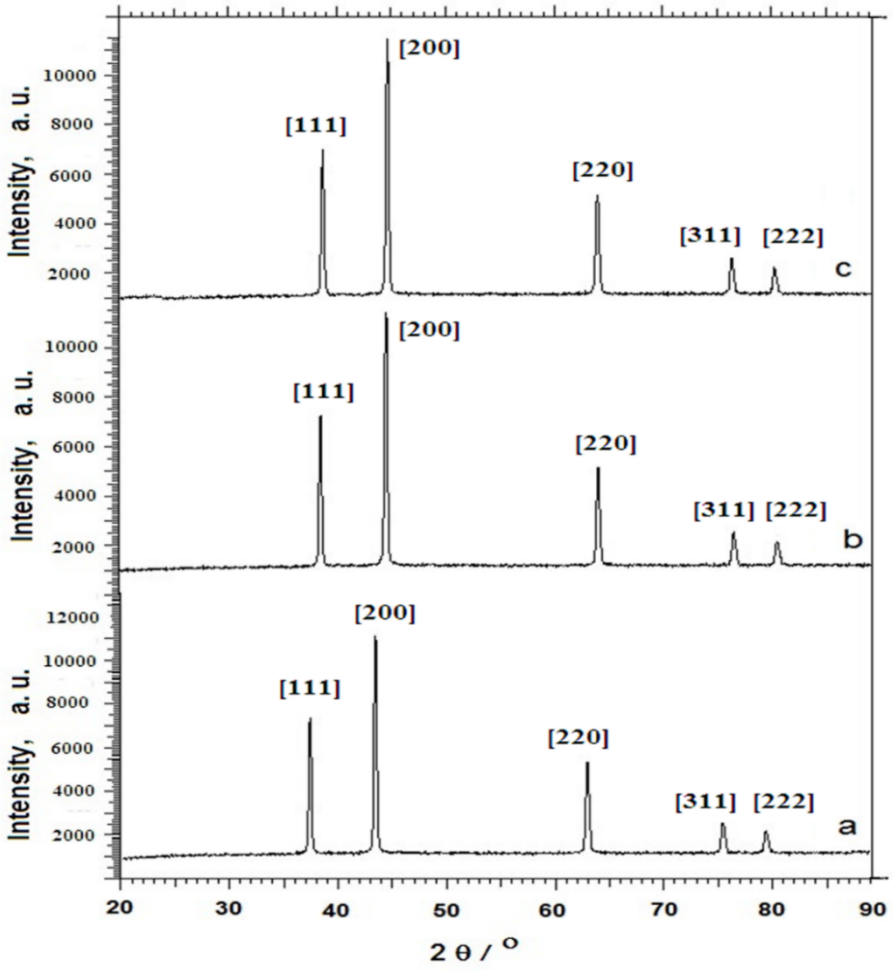

Fig. 4. XRD diagrams of (a) nano-NiO particles; (b) nano-NiO coated by palmitic acid; (c) nano-NiO particles coated by stearic acid.

In Figs. 4a and 4b observed that the characteristic angles did not change after coating the surface using fatty acids, and the angles are the same as those observed in nano-nickel oxide particles with fcc phase structure. The intensity signals of the XRD pattern showed that nano-NiO particles were highly crystalline. Average sizes of nickel oxide and nano-NiO particles coated using palmitic and stearic acids that were determined from XRD patterns and the Debye-Sherrer formula (Eq. 4):

$$D = \frac{K.\lambda}{\beta.\cos\theta} \quad (4)$$

were 80 and 95 nm respectively. The constant value K, in the equation, is 0.89, the wavelength of the scattered light is 1.54 Å, and β means half the width of the highest signal.

The SEM pictures and EDX spectra

Nanomaterials tend to be agglomerated and aggregated because of their high surface energy.

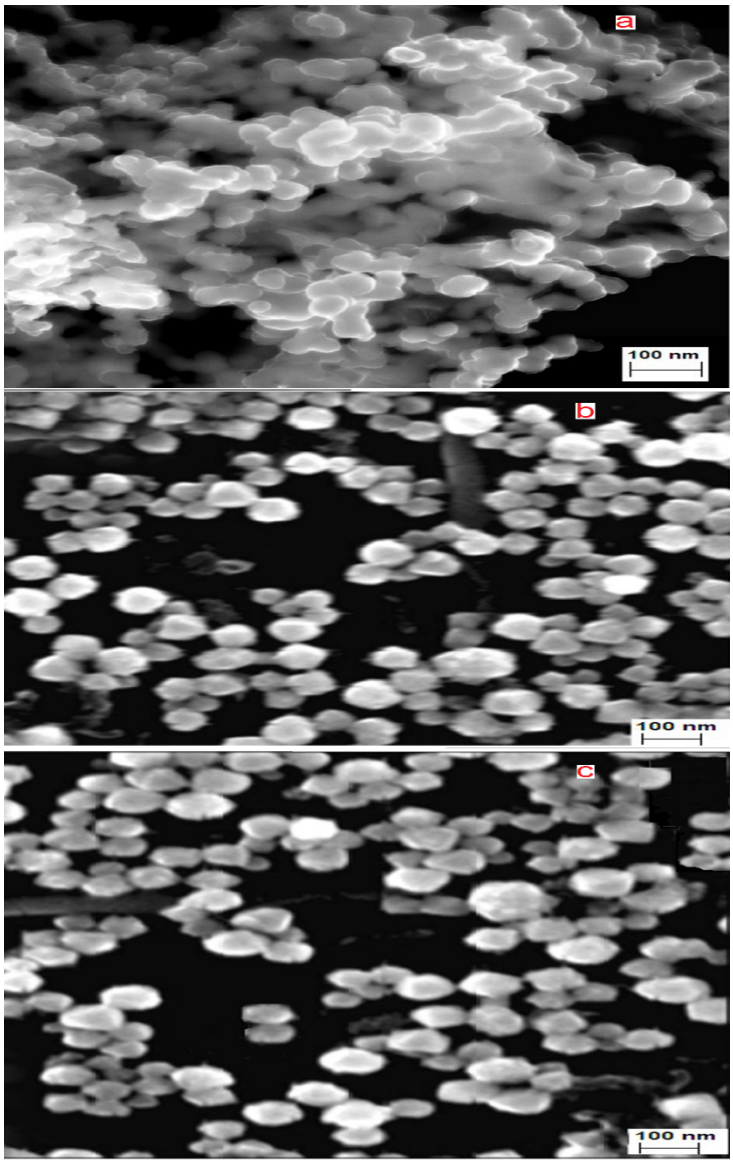

Fig. 5. The SEM pictures of (a) uncoated nano-NiO particles, (b) the nano-NiO particles coated by palmitic acid, and (c) the nano-NiO particles coated by stearic acid.

Therefore, coatings on their surface are expected to reduce agglomeration and aggregation and improve their dispersibility. For the study of particle morphology and dispersion, SEM pictures of nanomaterials samples were recorded before and after coating using stearic and palmitic acids, and these pictures are shown in Fig. 5.

As seen in Fig. 5a, the uncoated nano-NiO particles are strongly agglomerated. The dispersion of the particles improved with its surface coated using stearic and palmitic acids and the particles became slightly larger (Figs. 5b and 5c). This improvement in the dispersion of the nanomaterials confirms once again that the surface of nickel oxide is coated using palmitic and stearic acids. The average sizes of nano-NiO particles and nickel oxide coated by palmitic and stearic acids in SEM pictures are 95 and 100 nm, respectively. The values obtained have good compatibility with particle size determined from the XRD patterns.

The EDX analysis of nano-NiO particles and nickel oxide coated using stearic acid (SA) are displayed in Fig. 6. The EDX analysis in Fig. 6a showed nickel and oxygen as the only elements present in nano-NiO particles. The presence of nickel, oxygen, and carbon atoms in coated nano-NiO particles (Fig. 6b) proves that the surface of nickel oxide was coated using stearic acid (SA).

TGA thermograms

TGA thermogram can be used to affirm the incorporation of a certain number of fatty acids on the superface of nickel oxide. The TGA thermograms of nickel oxide and its coated by palmitic and stearic acids are shown in Fig. 7. There is a weight loss of 4.7 % when uncoated nano-NiO particles are heated from 215 to 430 ºC, which can be imputed to the outflow of absorbed water (Fig. 7a). The nano-NiO particles coated using palmitic acid (PA) loss weight by 6.8 % when the temperature changed from 270 to 420 ºC, which can be related to the removal of surface water, and the burning of palmitic acid (PA) on the surface of coated nano-NiO particles (Fig. 7b). A similar performance was seen in nano-NiO particles coated using stearic acid (SA), with a mass loss of 7.4 %, when the temperature changed from 240 to 410 ºC (Fig. 7c). Compared to uncoated nano-NiO particles, the mass loss of nano-NiO particles showed that the amounts of palmitic acid (PA) and stearic acid (SA) incorporation were 2.1 and 2.7%, respectively.

The effective factors on LD

The lipophilic degree (LD) of the coated nano-NiO particles was employed in good circumstances for the superficial coating of the nickel oxide nanomaterials. To achieve this goal, different

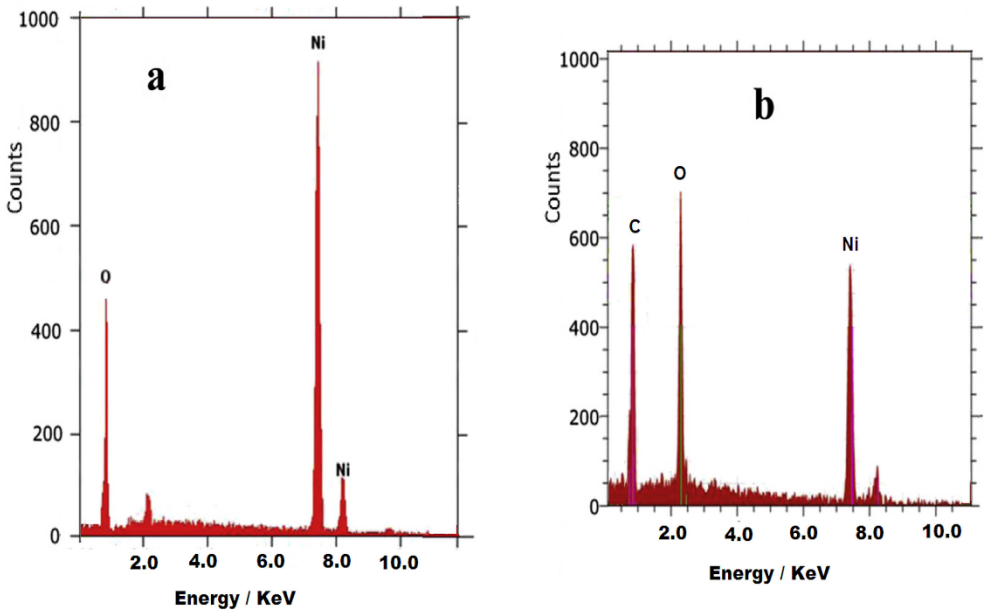

Fig. 6. The EDX diagrams of (a) nano-NiO particles, and (b) nano-NiO particles coated by stearic acid.

agents namely reaction temperature and time, and the amount of coating agent was considered. The outcomes showed that LD increased as long as the content of the coating agent on the surface of the particle is increased to 5 wt%. The optimal conditions of surface coating nanomaterials were also achieved at 35 ºC and 150 min for contact time.

Dispersity of the modified NiO NPs

The use of modified NPs applied processes depends very much on the suitability of the environment. Therefore, to find the best conditions it was planned to test the dispersity of surface-modified NPs in different solvents. To do this, a certain number of nano-NiO particles coated using palmitic and stearic acids were dispersed in each of the organic solvents such as ethanol, acetone, and liquid paraffin. The primary weight percentage of the coated nano-NiO particles varied from 2.5 to 20 %wt. The samples were then incubated at the environment temperature for three days. The sediment portion of particles was separated and the value of the stable particles in dispersion was measured gravimetric method (%wt). These outcomes are displayed in Table 2.

As shown in the above table, these results indicate the majority of coated nano-NiO particles precipitate in ethanol; while coated particles formed a stable dispersion in liquid paraffin. This is a good indication of the compatibility of nano-NiO particles coated with organic environments. Also,

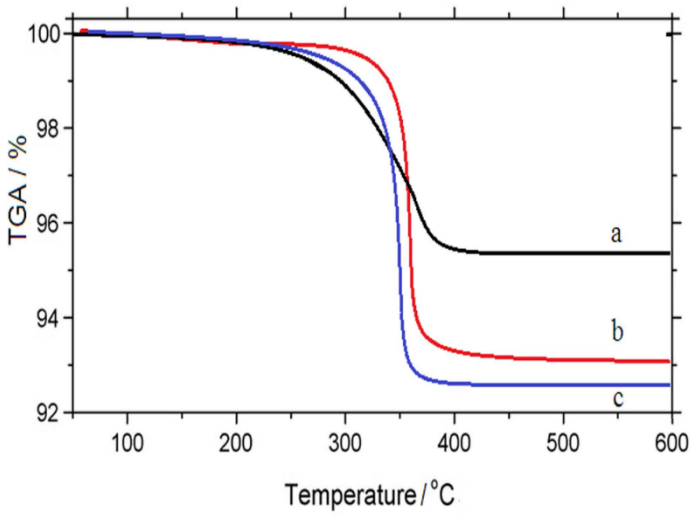

Fig. 7. The TGA thermograms of (a) nano-NiO particles; (b) nano-NiO particles coated by palmitic acid; (c) nano-NiO particles coated by stearic acid.

Table 2. Dispersion of nano-NiO particles modified by stearic (ST) and palmitic (PA) acids in several organic solvents (% wt).

Initial weight percent nano-NiO,[% wt]	Dispersion in ethanol , [% wt]		Dispersion in acetone, [% wt]		Dispersion in liquid paraffin , [% wt]	
	ST	PA	ST	PA	ST	PA
2.5	0.51	0.62	1.71	1.95	2.05	2.11
5	1.12	1.25	3.15	3.25	3.96	4.04
10	2.24	2.53	6.41	6.44	8.14	8.25
15	3.36	3.39	10.38	10.41	11.92	12.11
20	4.88	4.96	11.79	11.85	15.75	16.08

the organic chains bound to the surface of nano-NiO particles create repulsive forces between particles and therefore prevent agglomeration and aggregation [47]. Moreover, the hydrophilic surface of nano-NiO particles changes drastically and now becomes hydrophobic. So, surface modification can prevent aggregation, and improve dispersion in organic media.

Photocatalytic de-activities

The UV–Visible spectra of bare and stearic-capped nano-NiO particles dispersed in ethanol are shown in Fig. 8. These peaks at 370 nm and/ or 355 nm are assigned to intrinsic bandgap absorption of nickel oxide owing to electron jump from the valence to the conduction band ($O_{2p} \rightarrow Ni_{3d}$). The sharp signal denotes that the particles are in the nano dimension and the size distribution is narrow [82]. Therefore, nano-NiO particles prepared by this method could be a promising photocatalytic material.

The optical band gap was suggested by Tuac's equations [83]: $(\alpha h\nu)^2 = A(h\nu - E_g)$, where hv, α, and A are the photon energy, absorbency constant, and a constant relative to the compound, respectively. The plots of $(\alpha h\nu)^2$ against hv for nano-NiO

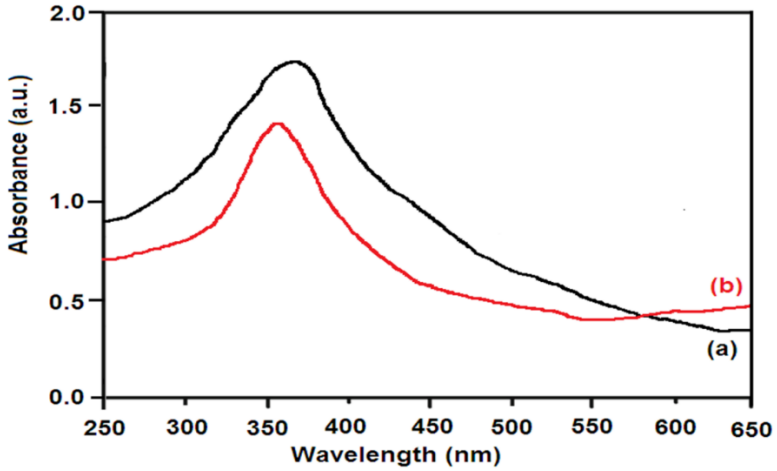

Fig. 8. The UV–Visible spectra of (a) nano-NiO particles, and (b) nano-NiO particles coated by stearic acid.

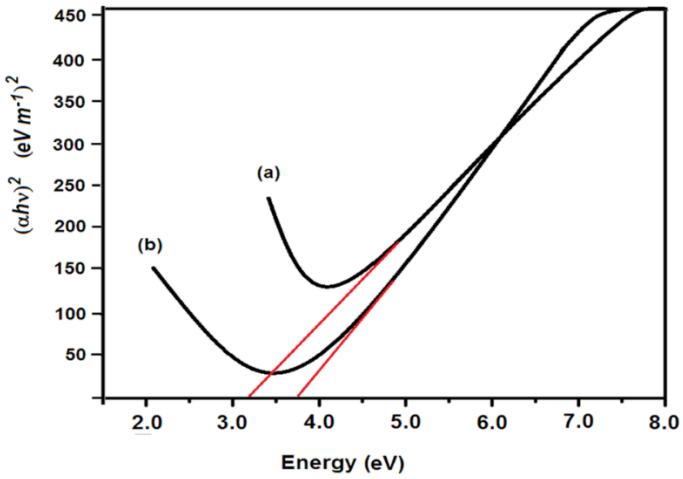

Fig. 9. The optical band gap plot of (a) nano-NiO particles, and (b) nano-NiO particles coated by stearic acid.

particles have been produced, from which a direct bandgap was found (Fig. 9).

Through the extrapolation on the linear region of this curve, the bandgap was estimated to be about 3.26 eV for bare NiO NPs and 3.75 eV for stearic-capped NiO NPs. Such an increase in the bandgap may correspond to the quantum confinement effect created by the stearic surfactant [84]. These bandgap values suggest that nano-NiO particles are a semiconductor. This value of E_g is in the same range where highly efficient photocatalytic materials are located. The resultant values of E_g of NiO NPs are found to be less than that obtained by the Salavati-Niasari group [85, 86]; this may be due to the preparation method used.

The photocatalytic behavior of nano-NiO particles was examined in the destruction of MO by UV light at various times (Fig. 10). By determining the absorbance at λ_{max}=464 nm for various times (2, 4, 6, and 8 h) PDP was determined from Eq. 2.

As seen in Fig. 10, the absorption of methyl orange decreases with prolonged irradiation. This indicates the molecular structure of MO is destroyed in the solution containing nano-nickel oxide particles under ultraviolet irradiation. The utmost absorption of MO at wavelength 464 nm

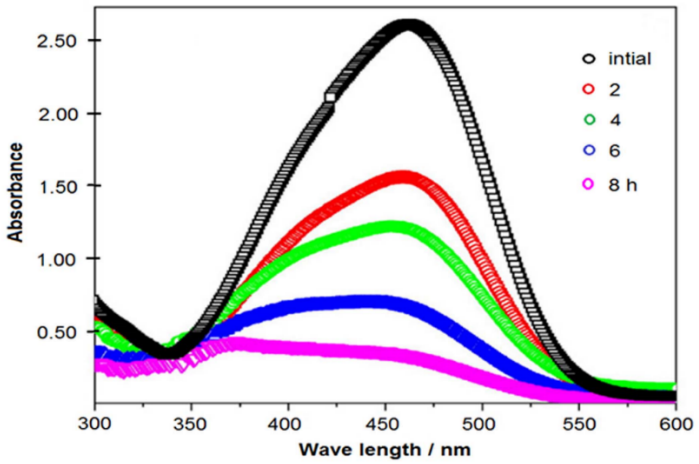

Fig. 10. The UV-Vis diagrams of MO in the presence of nano-NiO particles at different times under ultraviolet irradiation.

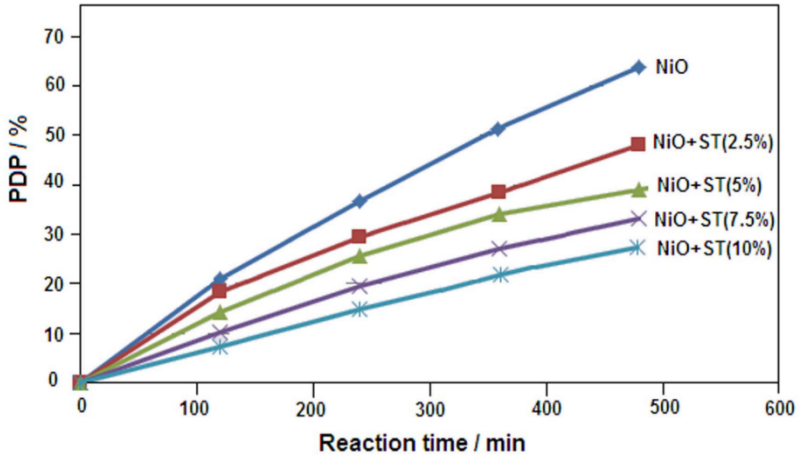

Fig. 11. The PDP of methyl orange in the vicinity of nano-NiO particles and its coated by stearic acid against UV light time.

Table 3. Destruction percentage of MO using nanoparticles under UV irradiated.

Nanoparticles	Photodegradation Percentage/%	Time reaction/h	References
ZnO	80	4	42
ZnO-Polystyrene	0		
ZnO	95	6	41
ZnO-Polystyrene	0		
CuO	62	8	31
CuO-Stearic acid	18		
NiO	65	8	This work
NiO-Stearic acid	27		

owing to the azo group in its molecular structure [87]. Therefore, the decrease in absorption for MO is because of the destruction of the azo bond after that the color of the media disappears.

In the next test, the absorbance of the solution was determined at the primary value of 10 ppm methyl orange, and various amounts of nano-NiO particles coated using stearic acid (2.5, 5, 7.5, and 10 % wt) by UV light at various times (2, 4, 6 and 8 h). Afterward, PDP was determined and the results were plotted as the percentage of MO destruction against irradiance time (Fig. 11).

As seen in Fig. 11, the uncoated nano-NiO particles have the highest photocatalytic activity; whereas the nanoparticles coated using stearic acid have a lower photocatalytic operation. This is because nano-NiO particles have a hydrophilic character and can absorb more MO from the aqueous media. This, in turn, increases the effective contact and the ultraviolet light engenders hole-electron pairs on nano-NiO particles which produce active hydroxyl radicals and destroys methyl orange in an aqueous solution [62, 88].

The nano-NiO particles coated using stearic acid are hydrophobic and become floated on the methyl orange solution. So, fewer hydroxyl radicals are generated, which subsequently results in less MO being lost [88]. In addition, UV absorption of nano-NiO particles can be decreased owing to coated stearic layers [87]. Similarly, this process also results in fewer hydroxyl radicals being formed, thereby reducing the photocatalytic behavior of nano-NiO particles [88-90].

At last, by increasing the amount of the modifier, the thickness of the organic layers increases with the hydrophobic nature. Subsequently, the buoyant on the MO solution increased and the photocatalytic destruction decreased [62]. However, the internal surface of nano-NiO particles is fully active and produces hole-electron pairs by ultraviolet irradiation, but they cannot present their route to the external surface of coated nano-nickel oxide particles. Thus, they cannot interact effectively with the solution [44, 88, 91].

In carbon compounds attached to the surface of nano-NiO particles, such as stearic acid (SA) and palmitic acid (PA), which do not have delocalized π-electrons and are not electrically conductive, electron relay does not occur and the photocatalytic activity of nano-NiO particles decreases [37, 44, 47]. While the carbon atoms attached to the surface of nano-NiO particles, such as RGO, which have delocalized π-electrons and are electrically conductive, the electron relay is performed well and the photocatalytic activity of nano-NiO particles increases [56-58].

The PDP of bare nano-nickel oxide particles and their coated with stearic acid are quite different under similar laboratory conditions. The destruction performance of nano-nickel oxide particles is decreased after coating using stearic acid. PDP of MO was decreased by 65% for eight hours in the presence of nano-NiO particles, while it was reduced by 27% in the vicinity of nano-NiO particles coated using stearic acid.

A few similar works to ours were reported in which methyl orange (MO) was degraded by nanoparticles under UV-irradiated. The destruction percentage of MO by various nanoparticles under ultraviolet light is shown in Table 3.

As can be seen, the photocatalytic activity of the nanoparticles decreases when their surface is covered by the capping agents. Bare NiO nanoparticles have higher photocatalytic performance because about 65% of MO was destroyed after 8 h. In contrast, stearic acid-grafted NiO NPs, which are hydrophobic, levitate on the MO solution and were approximately 27% of MO

degraded. However, degradation is not observed if the surficial of the particles is decorated by a polymer that has a long chain.

CONCLUSION

The nano-NiO particles were prepared by the green route from the interaction of $Ni(NO_3)_2.6H_2O$ and garlic extract and then heated at 400 °C for five hours. The hydrophilic character of the surficial nano-NiO particles was converted to a hydrophobic nature by coating them with palmitic and stearic acids. The presence of long-chain carboxylic acids on nano-NiO particles was confirmed using FT-IR analysis, and the results showed that palmitic and stearic acids were connected on nano-NiO particles via carboxylate form. The change like the surface of nano-NiO particles was also proved by the percentage of lipophilicity test. These outcomes showed that LD increases by the rise of coating value up to 5 wt% for palmitic and stearic acids. Optimal conditions for surface coating of nano-NiO particles were also achieved at 35 ºC and 150 min for reaction time. The dispersion of coated nano-NiO particles in organic solvents was investigated. The examined results revealed that the lowest dispersity for modified nano-NiO particles occurred in ethanol and the highest in liquid paraffin. The lipophilicity and stability of coated nano-NiO particles were increased in organic media without any change in their structure. TGA analysis for nano-NiO particles showed that palmitic and stearic acids incorporation rates were 2.1 and 2.7 wt%, respectively. The photocatalytic performances of nano-NiO particles and they are modified were determined in the destruction of MO. These outcomes showed that the catalytic performance of nano-NiO particles decreases when it is coated using stearic acid.

ACKNOWLEDGMENT

The authors would like to thank the Research Council of the Shahrood University of Technology for the financial support of this work.

CONFLICT OF INTEREST

The authors declare that there is no conflict of interests regarding the publication of this manuscript.

REFERENCES

1. Khan MM, Adil SF, Al-Mayouf A. Metal oxides as photocatalysts. Journal of Saudi Chemical Society. 2015;19(5):462-464.
2. Mousavi SM, Chamack M, Fakhri H. Study of new hybrid material of ZnO/CuO and metal-organic framework as photocatalyst for removal of tetracycline from water. Journal of Nanostructures, 2022;12:1097-1107.
3. Jolaei S, Mirzaei M, Hassanpour A, Safardoust H, Khani A. Using ZnO, NiO, and ZnO/NiO as nano photocatalyst for removal of acid violet and rhodamine B from wastewater. Journal of Nanostructures, 2022;12:761-770.
4. Aboud KH, AL-Jawad SMH, Imran NJ. Preparation and characterization of hierarchical CdS nanoflowers for efficient photocatalytic degradation. Journal of Nanostructures, 2022;12:316-329.
5. Raja VR, Muthupandi K, Karthika A, Aravindhan B, Nithya L. Preparation and characterization of NiO-WO3 nanocomposite with enhanced photocatalytic activity under visible light irradiation. Journal of Nanostructures, 2022;12:53-365.
6. Jalil AT, Al-Qurabiy HE, Dilfy SH, Meza SO, Aravindhan S, Kadhim MM, Aljeboree AM. CuO/ZrO_2 nanocomposites: Facile synthesis, characterization and photocatalytic degradation of tetracycline antibiotic. Journal of Nanostructures, 2021;11:333-346.
7. Salavati-Niasari M, Farhadi-Khouzani M, Davar F. Bright blue pigment $CoAl_2O_4$ nanocrystals prepared by modified sol–gel method. J Sol-Gel Sci Technol. 2009;52(3):321-327.
8. Salavati-Niasari M. Bright blue pigment $CoAl_2O_4$ nanocrystals prepared by modified sol–gel method. Journal of Sol-Gel Science and Technology, 2009;52(3):321-327.
9. Mousavi-Kamazani M, Zarghami Z, Salavati-Niasari M. Facile and Novel Chemical Synthesis, Characterization, and Formation Mechanism of Copper Sulfide (Cu_2S, Cu_2S/CuS, CuS) Nanostructures for Increasing the Efficiency of Solar Cells. The Journal of Physical Chemistry C. 2016;120(4):2096-2108.
10. Mohandes F, Salavati-Niasari M. Freeze-drying synthesis, characterization and in vitro bioactivity of chitosan/graphene oxide/hydroxyapatite nanocomposite. RSC Advences, 2014;4:25993-26001.
11. Zinatloo-Ajabshir S, Salavati-Niasari M. Nanocrystalline Pr_6O_{11}: synthesis, characterization, optical and photocatalytic properties. New J Chem. 2015;39(5):3948-3955.
12. Salavati-Niasari M, Davar F, Loghman-Estarki MR. Controllable synthesis of thioglycolic acid capped ZnS(Pn)0.5 nanotubes via simple aqueous solution route at low temperatures and conversion to wurtzite ZnS nanorods via thermal decompose of precursor. J Alloys Compd. 2010;494(1-2):199-204.
13. Mohandes F, Davar F, Salavati-Niasari M. Magnesium oxide nanocrystals via thermal decomposition of magnesium oxalate. Journal of Physics and Chemistry of Solids. 2010;71(12):1623-1628.
14. Davar F, Salavati-Niasari M, Mir N, Saberyan K, Monemzadeh M, Ahmadi E. Thermal decomposition route for synthesis of Mn3O4 nanoparticles in presence of a novel precursor. Polyhedron. 2010;29(7):1747-1753.
15. Safardoust-Hojaghan H, Salavati-Niasari M. Degradation of methylene blue as a pollutant with N-doped graphene quantum dot/titanium dioxide nanocomposite. Journal of Cleaner Production. 2017;148:31-36.
16. Yousefi M, Gholamian F, Ghanbari D, Salavati-Niasari M. Polymeric nanocomposite materials: Preparation and

characterization of star-shaped PbS nanocrystals and their influence on the thermal stability of acrylonitrile–butadiene–styrene (ABS) copolymer. Polyhedron. 2011;30(6):1055-1060.
17. Mir N, Salavati-Niasari M, Davar F. Preparation of ZnO nanoflowers and Zn glycerolate nanoplates using inorganic precursors via a convenient rout and application in dye sensitized solar cells. Chem Eng J. 2012;181-182:779-789.
18. Zinatloo-Ajabshir S, Morassaei MS, Salavati-Niasari M. Eco-friendly synthesis of $Nd_2Sn_2O_7$–based nanostructure materials using grape juice as green fuel as photocatalyst for the degradation of erythrosine. Composites Part B: Engineering. 2019;167:643-653.
19. Salavati-Niasari M. Ship-in-a-bottle synthesis, characterization and catalytic oxidation of styrene by host (nanopores of zeolite-Y)/guest ([bis(2-hydroxyanil) acetylacetonato manganese(III)]) nanocomposite materials (HGNM). Microporous Mesoporous Mater. 2006;95(1-3):248-256.
20. Njagi EC, Huang H, Stafford L, Genuino H, Galindo HM, Collins JB, Hoag GE, Suib SL. Biosynthesis of iron and silver nanoparticles at room temperature using aqueous Sorghum Bran extracts. Langmuir, 2011; 27(1):264–271.
21. Fardood ST, Ramazani A. Green synthesis and characterization of copper oxide nanoparticles using coffee powder extract. Journal of Nanostructures, 2016; 6:67-171.
22. Singh J, Dutta T, Kim K-H, Rawat M, Samddar P, Kumar P. Green' synthesis of metals and their oxide nanoparticles: Applications for environmental remediation. Journal of Nanobiotechnology, 2018;16:84.
23. Pansambal S, Deshmukh K, Savale A, Ghotekar S, Pardeshi, Jain G, Aher Y, Pore D. Phyto-synthesis and biological activities of fluorescent CuO nanoparticles using Acanthospermum hispidum L. extract. Journal of Nanostructures, 2017;7(3):165-174.
24. Nasrollahzadeh M, Sajadi SM, Khalaj M. Green synthesis of copper nanoparticles using aqueous extract of the leaves of Euphorbia esula L and their catalytic activity for ligand-free Ullmann-coupling reaction and reduction of 4-nitrophenol. RSC Adv. 2014;4(88):47313-47318.
25. Modi S, Fulekar MH. Green synthesis of zinc oxide nanoparticles using garlic skin extract and its characterization. Journal of Nanostructures, 2020; 10:20-27.
26. Arabi M, Ghaedi M, Ostovan A. Development of a Lower Toxic Approach Based on Green Synthesis of Water-Compatible Molecularly Imprinted Nanoparticles for the Extraction of Hydrochlorothiazide from Human Urine. ACS Sustainable Chemistry & Engineering. 2017;5(5):3775-3785.
27. Ramanathan S, Gopinath SCB, Anbu P, Lakshmipriya T, Kasim FH, Lee C-G. Eco-friendly synthesis of Solanum trilobatum extract-capped silver nanoparticles is compatible with good antimicrobial activities. J Mol Struct. 2018;1160:80-91.
28. Horníčková J, Velíšek J, Ovesná J, Stavělíková H. Distribution of S-alk(en)yl-l-cysteine Sulfoxides in Garlic (Allium sativum L.). Czech Journal of Food Sciences. 2009;27(Special Issue 1):S232-S235.
29. Kamenetsky R, London Shafir I, Khassanov F, Kik C, van Heusden AW, Vrielink-van Ginkel M, et al. Diversity in fertility potential and organo-sulphur compounds among garlics from Central Asia. Biodiversity and Conservation. 2005;14(2):281-295.
30. Lu X, Ross CF, Powers JR, Aston DE, Rasco BA. Determination of Total Phenolic Content and Antioxidant Activity of Garlic (Allium sativum) and Elephant Garlic (Allium ampeloprasum) by Attenuated Total Reflectance–Fourier Transformed Infrared Spectroscopy. Journal of Agricultural and Food Chemistry. 2011;59(10):5215-5221.
31. Luque-Morales PA, Lopez-Peraza A, Nava-Olivas OJ, Amaya-Parra G, Baez-Lopez YA, Orozco-Carmona VM, et al. ZnO Semiconductor Nanoparticles and Their Application in Photocatalytic Degradation of Various Organic Dyes. Materials. 2021;14(24):7537.
32. Chen S, Liu W. Preparation and Characterization of Surface-Coated ZnS Nanoparticles. Langmuir. 1999;15(23):8100-8104.
33. Wang Y, Eli W, Zhang L, Gao H, Liu Y, Li P. A new method for surface modification of nano-$CaCO_3$ and nano-Al_2O_3 at room temperature. Adv Powder Technol. 2010;21(2):203-205.
34. Liu Z, Yao L, Pan X, Liu Q, Huang H. A green and facile approach to the efficient surface modification of alumina nanoparticles with fatty acids. Appl Surf Sci. 2018;447:664-672.
35. Feng L, Zhang H, Mao P, Wang Y, Ge Y. Superhydrophobic alumina surface based on stearic acid modification. Appl Surf Sci. 2011;257(9):3959-3963.
36. Hong R, Pan T, Qian J, Li H. Synthesis and surface modification of ZnO nanoparticles. Chem Eng J. 2006;119(2-3):71-81.
37. Wu L, Zhang Y, Yang G, Zhang S, Yu L, Zhang P. Tribological properties of oleic acid-modified zinc oxide nanoparticles as the lubricant additive in poly-alpha olefin and diisooctyl sebacate base oils. RSC Advances. 2016;6(74):69836-69844.
38. Mariño F, López ER, Arnosa Á, González Gómez MA, Piñeiro Y, Rivas J, et al. ZnO nanoparticles coated with oleic acid as additives for a polyalphaolefin lubricant. J Mol Liq. 2022;348:118401.
39. Cao Z, Zhang Z. Deactivation of photocatalytically active ZnO nanoparticle and enhancement of its compatibility with organic compounds by surface-capping with organically modified silica. Appl Surf Sci. 2011;257(9):4151-4158.
40. Yu M, Yang L, Yan L, Wang T, Wang Y, Qin Y, et al. ZnO nanoparticles coated and stearic acid modified superhydrophobic chitosan film for self-cleaning and oil–water separation. Int J Biol Macromol. 2023;231:123293.
41. Sbardella F, Rivilla I, Bavasso I, Russo P, Vitiello L, Tirillò J, Sarasini F. Zinc oxide nanostructures and stearic acid as surface modifiers for flax fabrics in polylactic acid biocomposites. Int J Biol Macromol. 2021;177:495-504.
42. Agrawal N, Munjal S, Ansari Mohd Z, Khare N. Superhydrophobic palmitic acid modified ZnO nanoparticles. Ceram Int. 2017;43(16):14271-14276.
43. Nam S-H, Boo J-H. Growth and surface treatment of TiO_2 nanorods using stearic acid solution. Thin Solid Films. 2013;546:35-37.
44. Zhao J, Milanova M, Warmoeskerken MMCG, Dutschk V. Surface modification of TiO_2 nanoparticles with silane coupling agents. Colloids Surf Physicochem Eng Aspects. 2012;413:273-279.
45. Li Z, Bai L, Xing Z, Yang W, Wu Q, Zhang G. Stearic acid-TiO2 composite Janus sheets perpendicular to the interface for emulsification and photocatalysis. Inorg Chem Commun. 2022;144:109835.
46. Yuan Z, Chen H, Li C, Huang L, Fu X, Zhao D, Tang J. Facile

method to prepare stable superhydrophobic Co3O4 surface. Appl Surf Sci. 2009;255(23):9493-9497.
47. Soleimani E, Taheri R. Synthesis and surface modification of CuO nanoparticles: Evaluation of dispersion and lipophilic properties of modified nanoparticles. Nano–Structures & Nano–Objects, 2017;10:167–175.
48. Singh AP, Dwivedi RK, Kumar R, Agarwal A, Suhane A. Study of oleic acid as a surface modifying agent for oxide nanoparticles. Materials Today: Proceedings. 2022;62:6550-6553.
49. Deraz NM, Selim MM, Ramadan M. Processing and properties of nanocrystalline Ni and NiO catalysts. Materials Chemistry and Physics. 2009;113(1):269-275.
50. Li F, Chen H-y, Wang C-m, Hu K-a. A novel modified NiO cathode for molten carbonate fuel cells. J Electroanal Chem. 2002;531(1):53-60.
51. Hotovy I, Huran J, Spiess L, Hascik S, Rehacek V. Preparation of nickel oxide thin films for gas sensors applications. Sensors and Actuators B: Chemical, 1999;57:147–152.
52. Ahmad T, Ramanujachary KV, Lofland SE, Ganguli AK. Magnetic and electrochemical properties of nickel oxide nanoparticles obtained by the reverse-micellar route. Solid State Sciences. 2006;8(5):425-430.
53. Borgström M, Blart E, Boschloo G, Mukhtar E, Hagfeldt A, Hammarström L, Odobel F. Sensitized Hole Injection of Phosphorus Porphyrin into NiO: Toward New Photovoltaic Devices. The Journal of Physical Chemistry B. 2005;109(48):22928-22934.
54. Sasi B, Gopchandran KG. Nanostructured mesoporous nickel oxide thin films. Nanotechnology. 2007;18(11):115613.
55. Sasi B, Gopchandran KG, Manoj PK, Koshy P, Prabhakara Rao P, Vaidyan VK. Preparation of transparent and semiconducting NiO films. Vacuum. 2002;68(2):149-154.
56. Shanmugam V, Mohan S, Manimaran P, Ravikumar K, Chandekar KV, Ben Gouider Trabelsi A, et al. Hydrothermal development of a novel NiO/rGO nanocomposites for dual supercapacitor and photocatalytic applications. Materials Chemistry and Physics. 2022;289:126425.
57. Vivek P, Sivakumar R, Selva Esakki E, Deivanayaki S. Fabrication of NiO/RGO nanocomposite for enhancing photocatalytic performance through degradation of RhB. Journal of Physics and Chemistry of Solids. 2023;176:111255.
58. Mokhtar A, Abdelkrim S, Boukoussa B, Hachemaoui M, Djelad A, Sassi M, Abboud M. Elimination of toxic azo dye using a calcium alginate beads impregnated with NiO/activated carbon: Preparation, characterization and RSM optimization. Int J Biol Macromol. 2023;233:123582.
59. Hong RY, Chen LL, Li JH, Li HZ, Zheng Y, Ding J. Preparation and application of polystyrene-grafted ZnO nanoparticles. Polym Adv Technol. 2007;18(11):901-909.
60. Hong RY, Li JH, Chen LL, Liu DQ, Li HZ, Zheng Y, Ding J. Synthesis, surface modification and photocatalytic property of ZnO nanoparticles. Powder Technol. 2009;189(3):426-432.
61. Soleimani E, Mohammadi M. Synthesis, characterization and properties of polystyrene/NiO nanocomposites. Journal of Materials Science: Materials in Electronics. 2018;29(11):9494-9508.
62. Zhang L, An L, Liu B, Yang H. Synthesis and photocatalytic activity of porous polycrystalline NiO nanowires. Appl Phys A. 2011;104(1):69-75.
63. Pourtaheri A, Nezamzadeh-Ejhieh A. Enhancement in photocatalytic activity of NiO by supporting onto an Iranian clinoptilolite nano-particles of aqueous solution of cefuroxime pharmaceutical capsule. Spectrochimica Acta Part A: Molecular and Biomolecular Spectroscopy. 2015;137:338-344.
64. Chen Y-C, Zheng F-C, Min Y-L, Wang T, Zhang Y-G, Wang Y-X. Facile procedure to synthesize highly crystalline Ag/NiO nanocomposite microspheres and their photocatalytic activity. Journal of Materials Science: Materials in Electronics. 2012;23(8):1592-1598.
65. Sreethawong T, Ngamsinlapasathian S, Yoshikawa S. Surfactant-aided sol–gel synthesis of mesoporous-assembled TiO_2–NiO mixed oxide nanocrystals and their photocatalytic azo dye degradation activity. Chem Eng J. 2012;192:292-300.
66. Ahmed MA. Synthesis and structural features of mesoporous NiO/TiO_2 nanocomposites prepared by sol–gel method for photodegradation of methylene blue dye. J Photochem Photobiol A: Chem. 2012;238:63-70.
67. Ali AM, Najmy R. Structural, optical and photocatalytic properties of NiO–SiO_2 nanocomposites prepared by sol–gel technique. Catal Today. 2013;208:2-6.
68. Wang Z. Iron complexes nanoparticles synthesized by eucalyptus leaves. ACS Sustainable Chemistry & Engineering, 2013;1(12):1551–1554.
69. Salar RK, Sharma P, Kumar N. Enhanced antibacterial activity of streptomycin against some human pathogens using green synthesized silver nanoparticles. Resource-Efficient Technologies. 2015;1(2):106-115.
70. Devika R, Elumalai S, Manikandan E, Eswaramoorthy D. Biosynthesis of silver nanoparticles using the Fungus Pleurotus ostreatus and their antibacterial activity. Open Access Scientific Reports, 2012; 1(12):557.
71. Kranner I, Colville L. Metals and seeds: Biochemical and molecular implications and their significance for seed germination. Environmental and Experimental Botany. 2011;72(1):93-105.
72. Soleimani E, Niavarzi FB. Preparation, characterization and properties of PMMA/NiO polymer nanocomposites. Journal of Materials Science: Materials in Electronics. 2017;29(3):2392-2405.
73. Adyani SH, Soleimani E. Green synthesis of Ag/Fe_3O_4/RGO nanocomposites by Punica Granatum peel extract: Catalytic activity for reduction of organic pollutants. Int J Hydrogen Energy. 2019;44(5):2711-2730.
74. Adyani SH, Soleimani E, Hossaini Z. Silver and copper–magnetite nanocomposites as green and magnetic recoverable catalysts for the preparation of cyclopentadiene derivatives from a tri-component condensation. Reaction Kinetics, Mechanisms and Catalysis. 2019;128(2):885-901.
75. Nasrollahzadeh M, Sajadi SM, Rostami-Vartooni A, Bagherzadeh M. Green synthesis of Pd/CuO nanoparticles by Theobroma cacao L. seeds extract and their catalytic performance for the reduction of 4-nitrophenol and phosphine-free Heck coupling reaction under aerobic conditions. Journal of Colloid and Interface Science. 2015;448:106-113.
76. Nasrollahzadeh M, Atarod M, Sajadi SM. Green synthesis of the Cu/Fe_3O_4 nanoparticles using Morinda morindoides leaf aqueous extract: A highly efficient magnetically separable catalyst for the reduction of organic dyes in aqueous medium at room temperature. Appl Surf Sci. 2016;364:636-644.

77. Alagiri M, Ponnusamy S, Muthamizhchelvan C. Synthesis and characterization of NiO nanoparticles by sol–gel method. Journal of Materials Science: Materials in Electronics. 2011;23(3):728-732.
78. Lee S-Y, Harris MT. Surface modification of magnetic nanoparticles capped by oleic acids: Characterization and colloidal stability in polar solvents. Journal of Colloid and Interface Science. 2006;293(2):401-408.
79. Ramos-González R, García-Cerda LA, Quevedo-López MA. Study of the surface modification with oleic acid of nanosized HfO2 synthesized by the polymerized complex derived sol–gel method. Appl Surf Sci. 2012;258(16):6034-6039.
80. Harraz FA, Mohamed RM, Shawky A, Ibrahim IA. Composition and phase control of Ni/NiO nanoparticles for photocatalytic degradation of EDTA. J Alloys Compd. 2010;508(1):133-140.
81. Han DY, Yang HY, Shen CB, Zhou X, Wang FH. Synthesis and size control of NiO nanoparticles by water-in-oil microemulsion. Powder Technol. 2004;147(1-3):113-116.
82. Khorsand Zak A, Razali R, Abd Majid WH, Darroudi M. Synthesis and characterization of a narrow size distribution of zinc oxide nanoparticles. International Journal of Nanomedicine, 2011;6:1399–1403.
83. Tauc J, Grigorovici R, Vancu A. Optical Properties and Electronic Structure of Amorphous Germanium. physica status solidi (b). 1966;15(2):627-637.
84. Sadjadi MS, Khalilzadegan A. The effect of capping agents, EDTA and Eg on the structure and morphology of CdS nanoparticles. Journal of Non–Oxide Glasses, 2015;7(4):55–63.
85. Davar F, Fereshteh Z, Salavati-Niasari M. Nanoparticles Ni and NiO: Synthesis, characterization and magnetic properties. J Alloys Compd. 2009;476(1-2):797-801.
86. Salavati-Niasari M, Davar F, Fereshteh Z. Synthesis of nickel and nickel oxide nanoparticles via heat-treatment of simple octanoate precursor. J Alloys Compd. 2010;494(1-2):410-414.
87. Ezhilarasi AA, Vijaya JJ, Kaviyarasu K, Kennedy LJ, Ramalingam RJ, Al-Lohedan HA. Green synthesis of NiO nanoparticles using Aegle marmelos leaf extract for the evaluation of in-vitro cytotoxicity, antibacterial and photocatalytic properties. Journal of Photochemistry and Photobiology B: Biology, 2018; 180:39-50.
88. Rajan PI, Vijaya JJ, Jesudoss SK, Kaviyarasu K, Kennedy LJ, Jothiramalingam R, et al. Green-fuel-mediated synthesis of self-assembled NiO nano-sticks for dual applications—photocatalytic activity on Rose Bengal dye and antimicrobial action on bacterial strains. Materials Research Express. 2017;4(8):085030.
89. Ezhilarasi AA, Vijaya JJ, Kennedy LJ, Kaviyarasu K. Green mediated NiO nano-rods using Phoenix dactylifera (Dates) extract for biomedical and environmental applications. Materials Chemistry and Physics. 2020;241:122419.
90. Park H, Park Y, Kim W, Choi W. Surface modification of TiO_2 photocatalyst for environmental applications. Journal of Photochemistry and Photobiology C: Photochemistry Reviews. 2013;15:1-20.
91. Fuku X, Matinise N, Masikini M, Kasinathan K, Maaza M. An electrochemically active green synthesized polycrystalline NiO/MgO catalyst: Use in photo-catalytic applications. Mater Res Bull. 2018;97:457-465.